Extrinsic Repair of Injured Dendrites as a Paradigm for Regeneration by Fusion in *Caenorhabditis elegans*

Meital Oren-Suissa,[1] Tamar Gattegno,[1] Veronika Kravtsov, and Benjamin Podbilewicz[2]

Department of Biology, Technion-Israel Institute of Technology, Haifa 32000, Israel

ORCID IDs: 0000-0001-9937-8326 (M.O.-S.); 0000-0002-0411-4182 (B.P.)

ABSTRACT Injury triggers regeneration of axons and dendrites. Research has identified factors required for axonal regeneration outside the CNS, but little is known about regeneration triggered by dendrotomy. Here, we study neuronal plasticity triggered by dendrotomy and determine the fate of complex PVD arbors following laser surgery of dendrites. We find that severed primary dendrites grow toward each other and reconnect via branch fusion. Simultaneously, terminal branches lose self-avoidance and grow toward each other, meeting and fusing at the tips via an AFF-1-mediated process. Ectopic branch growth is identified as a step in the regeneration process required for bypassing the lesion site. Failure of reconnection to the severed dendrites results in degeneration of the distal end of the neuron. We discover pruning of excess branches via EFF-1 that acts to recover the original wild-type arborization pattern in a late stage of the process. In contrast, AFF-1 activity during dendritic auto-fusion is derived from the lateral seam cells and not autonomously from the PVD neuron. We propose a model in which AFF-1-vesicles derived from the epidermal seam cells fuse neuronal dendrites. Thus, EFF-1 and AFF-1 fusion proteins emerge as new players in neuronal arborization and maintenance of arbor connectivity following injury in *Caenorhabditis elegans*. Our results demonstrate that there is a genetically determined multi-step pathway to repair broken dendrites in which EFF-1 and AFF-1 act on different steps of the pathway. EFF-1 is essential for dendritic pruning after injury and extrinsic AFF-1 mediates dendrite fusion to bypass injuries.

KEYWORDS EFF-1; AFF-1; dendrite auto-fusion; degeneration following dendrotomy; regeneration of dendritic trees

SENSORY perception relies on networks of neurons that monitor and modify behavior to assure that animals are able to locate food, sense their environment, and avoid predators or other threats (Goodman 2003). This perception depends on the integrity and spatial coverage of the receptive field (Hall and Treinin 2011). Axonal and dendritic trees play an essential role in processing and transducing information to ultimately evoke the appropriate response of the organism. In the central nervous system (CNS) of adult mammals, axon regeneration following injury is limited (Ruschel *et al.* 2015). Therefore, the regenerative process following axon severing has been the focus of numerous studies (Taylor *et al.* 2005;

Park *et al.* 2008; Ruschel *et al.* 2015). It is believed that the main reasons why axons fail to regenerate are a reduction in neuronal growth capacity and inhibitory extrinsic factors. However, the molecular mechanisms of regeneration are not well-understood. Recent studies have suggested that modulation of intrinsic neuronal activity by mammalian target of rapamycin (mTOR) and G-protein-coupled receptor (GPCR) signaling promote axon regeneration (Park *et al.* 2008; Li *et al.* 2016). In parallel, there is evidence for a molecular pathway for axonal degeneration that affects regeneration (Coleman and Freeman 2010). The molecular mechanisms required for regeneration by regrowth following axonal injury are actively studied and numerous pathways have been identified (Taylor *et al.* 2005; Wu *et al.* 2007; Park *et al.* 2008; Hammarlund *et al.* 2009; Yan *et al.* 2009; Edwards and Hammarlund 2014; Hammarlund and Jin 2014; Ruschel *et al.* 2015). In contrast to regeneration by regrowth, a different strategy for axonal regeneration that has been observed in diverse invertebrates is reconnection by fusion of severed axons (Hoy *et al.* 1967; Bedi and Glanzman 2001; Yanik *et al.* 2004; Ghosh-Roy and Chisholm 2010; Neumann *et al.* 2011, 2015).

The nematode *Caenorhabditis elegans* is a powerful model to study neuronal regeneration after injury (Chisholm *et al.* 2016; Giordano-Santini *et al.* 2016). It has been recently found that injured axons of motor and mechanosensory neurons regrow and, in some cases, fuse after *in vivo* severing using laser surgery (Yanik *et al.* 2004; Bourgeois and Ben-Yakar 2007; Ghosh-Roy and Chisholm 2010; Ghosh-Roy *et al.* 2010; Neumann *et al.* 2011; Giordano-Santini *et al.* 2016). Moreover, screens for genes with roles in axon regrowth have identified many genes required for axon regeneration (Gabel *et al.* 2008; Ghosh-Roy and Chisholm 2010; Nix *et al.* 2014; Chisholm *et al.* 2016).

Compared to axonal regeneration and degeneration pathways, much less is known about dendritic regeneration following injury (Standler and Bernstein 1982; Hall and Cohen 1988; Stone *et al.* 2010, 2014; Song *et al.* 2012). Recent studies have identified the PVD and FLP neurons as highly branched bilateral neurons in *C. elegans*, which display a stereotypic dendritic arborization pattern composed of repetitive structural units known as menorahs (Figure 1, A and B) (White *et al.* 1986; Yassin *et al.* 2001; Halevi *et al.* 2002; Tsalik *et al.* 2003; Oren-Suissa *et al.* 2010; Pujadas *et al.* 2010; Smith *et al.* 2010; Albeg *et al.* 2011; Maniar *et al.* 2012). The PVD is highly polarized, with a single axon ventral to the cell body and complex but stereotyped dendritic arbors (Oren-Suissa *et al.* 2010; Maniar *et al.* 2012), making it an ideal system to study different aspects of the generation, maintenance, regeneration, and degeneration of dendritic trees. The PVD neurons are two polymodal nociceptors, responsible for an avoidance response generated after harsh mechanical stimuli to the main body or exposure to cold temperatures (Way and Chalfie 1989; Goodman 2003; Chatzigeorgiou *et al.* 2010). Animals in which PVD neurons are laser-ablated fail to respond to harsh touch (Way and Chalfie 1989). Recent studies uncovered the degenerin ion channels DEG/ENaC, MEC-10, and DEGT-1 that sense harsh touch, and the TRPA-1 channels that respond to cold temperatures (Albeg *et al.* 2011; Chatzigeorgiou and Schafer 2011). Moreover, researchers have identified numerous genetic pathways involved in dendritic arborization and maintenance of the PVD structure (Oren-Suissa *et al.* 2010; Aguirre-Chen *et al.* 2011; Smith *et al.* 2012; Salzberg *et al.* 2013; Liang *et al.* 2015; Taylor *et al.* 2015; Dong *et al.* 2016).

The dynamic pathway of PVD arborization revealed a function of EFF-1 fusogenic protein in sculpting neuronal trees (Oren-Suissa *et al.* 2010). EFF-1 mediates epithelial and muscle cell-to-cell fusion (Mohler *et al.* 2002; Shemer *et al.* 2004; Gattegno *et al.* 2007; Shinn-Thomas and Mohler 2011; Podbilewicz 2014; Shinn-Thomas *et al.* 2016; Smurova and Podbilewicz 2016a,b), auto cell fusion in the digestive tract (Rasmussen *et al.* 2008), and axonal fusion following injury (Ghosh-Roy and Chisholm 2010; Ghosh-Roy *et al.* 2010; Neumann *et al.* 2011, 2015). EFF-1 cell-autonomous expression in the PVD is sufficient to reduce the number of branches and to rescue disorganized menorahs (Oren-Suissa *et al.* 2010). EFF-1 controls dendritic plasticity via retraction of excess branches, by fusing branches, and by forming loops that restrict further growth (Oren-Suissa *et al.* 2010). AFF-1, a paralog of EFF-1, mediates fusion of the anchor cell to form the utse/hymen, fuses the lateral epidermal seam cells, merges some embryonic epithelial cells (Sapir *et al.* 2007; Avinoam *et al.* 2011), and fuses cells to form the tail spike (Chiorazzi *et al.* 2013). AFF-1 also fuses glial cells (Procko *et al.* 2011), is induced by Notch to auto-fuse a myoepithelial toroid (Rasmussen *et al.* 2008), and fuses the excretory duct cell to form a single-cell tube (Stone *et al.* 2009; Soulavie and Sundaram 2016). Here, we determine a cellular pathway for dendritic remodeling following injury. We uncover the functions of two fusion proteins, EFF-1 and AFF-1, in different stages of the regeneration of dendritic arbors of the PVD polymodal neuron in *C. elegans*.

Materials and Methods

Strains and transgenic animals

All nematode strains were maintained according to standard protocols (Brenner 1974; Sulston and Hodgkin 1988). In addition to the wild-type strain N2, the following mutations, transgenes, and strains were used: BP601 *aff-1*(*tm2214*)/*mIn1*[*dpy-10*(*e128*) *mIs14*] *II* (Sapir *et al.* 2007), MF190 *hmIs4*[*DES-2*::*GFP*, *pRF4*], BP328 *eff-1*(*ok1021*) *II*; *hmIs4*, BP450 *hyEx30*[*myo-2*::*gfp*, *DES-2*::*GFP*, *KS*], BP431 *eff-1*(*hy21*) *II*; *hmIs4* (Oren-Suissa *et al.* 2010), NC1841 (*wdIs52*, *F49H12.4*::*gfp*; *rwIs1*, *pmec-7*::RFP) (Smith *et al.* 2010), and CHB392 [*hmnEx133*(*ser-2prom3*::*kaede*)], kindly provided by Yip and Heiman (2016). Germline transformation was performed using standard protocols (Mello and Fire 1995). The KS bluescript plasmid was used as carrier DNA. Transgenic lines include: BP709 [*hmnIs133* (*ser-2prom3*::*kaede*)]; BP1014 *aff-1*/*mln1*; *dzIs53*[*pF49H12.4*::*mCherry*]*Is* was created by crossing *aff-1*/*mln1* with *pF49H12.4*::*mCherry* (kindly provided by Y. Salzberg); BP1015 *aff-1*/*mln1*; *hmnIs133*[*ser-2prom3*::*kaede*]; *hyEx66* [*KS*, *pCFJ90* (*myo-2*::*mcherry*), *pME4*(*des-2*::*AFF-1*)]; BP1017 *aff-1*/*mln1*; *hmnIs133*[*ser-2prom3*::*kaede*]; *hyEx350*[*KS*, *pCFJ90 myo-2*::*mcherry*, *pTG5 dpy-7p*::*aff-1*]; BP1052 *aff-1*/*mln1*; *hmnIs133*[*ser-2prom3*::*kaede*]; *hyEx355*[*KS*, *pCFJ90 myo-2*::*mcherry*, *pTG4 grd-10p*::*aff-1*]; BP1055 *dzIs53*[*F49H12.4p*::*mCherry*]; *hyEx66*[*pRF4*, *AFF-1 fosmid*::*GFP*, *KS*]; and BP1056 *dzIs53*[*F49H12.4p*::*mCherry*]; *hyEx68*[*pRF4*, *AFF-1 fosmid*::*GFP*, *KS*].

Molecular biology

We used restriction-free cloning to insert the *grd-10* promoter upstream to the *aff-1* gene (Bond and Naus 2012), and Gateway cloning (Petersen and Stowers 2011) to clone *aff-1* into a plasmid containing the *dpy-7* promoter fragment (pDest Dpy7 and pDONR221). Phusion Hot Start II High-Fidelity DNA polymerase (Thermo Scientific, Waltham, MA) was used to facilitate the cloning process.

Confocal microscopy and live imaging of C. elegans

Nematodes were mounted on 3% agar pads mixed with 10 mM NaN_3 in M9 buffer. For time-lapse analysis, worms
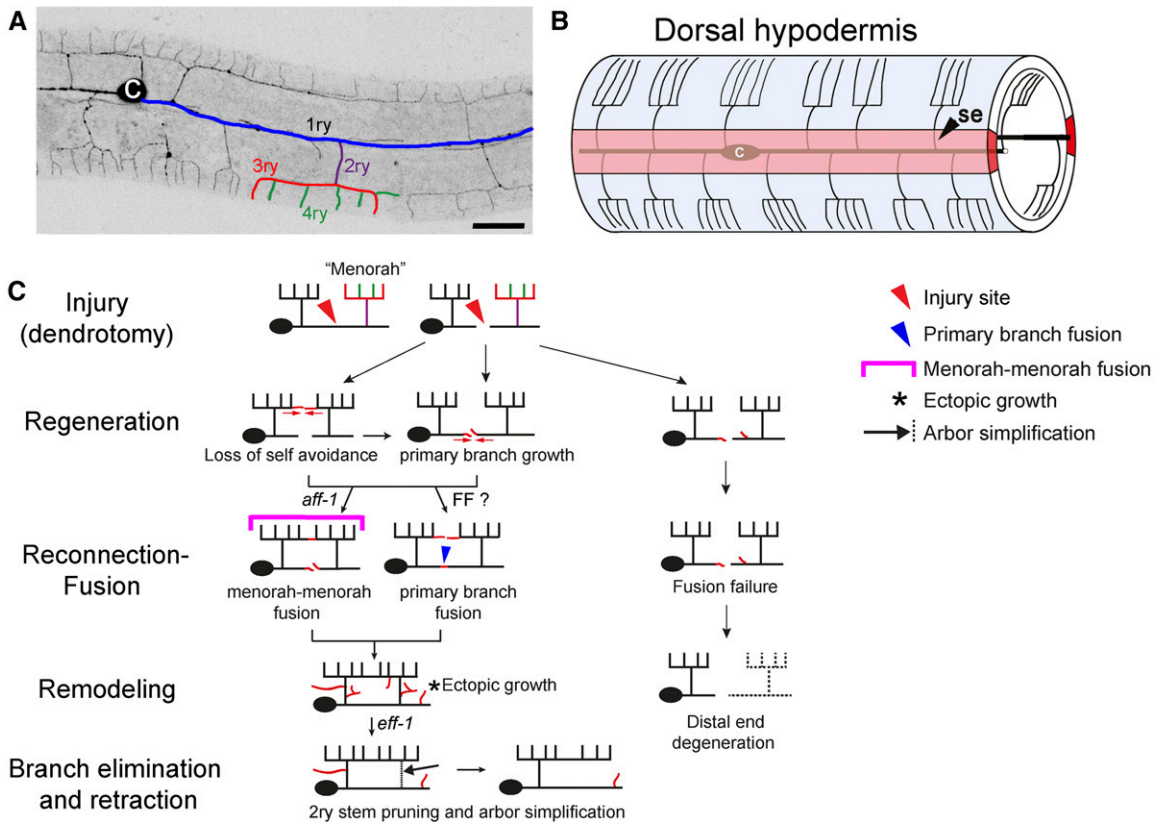
Figure 1 Dendrite regeneration of multibranched PVD neurons following laser microsurgery in *C. elegans*. (A) A wild-type animal expressing *DES-2*::*GFP*, illustrating the PVD neuron elaborate branching pattern (inverted image). Branches of one menorah are numbered primary to quaternary (1ry to 4ry) and color-coded: blue, purple, red, and green, respectively (Oren-Suissa *et al.* 2010); c, cell body. Bar, 20 μm. (B) Schematic model of hypodermal cells and PVD menorahs in a young adult, left view. The wild-type PVDs grow between the hypodermis (outer cylinder, light blue) and the basement membrane of the hypodermis (data not shown), extending processes that branch out to form the menorah structures. In light red is the left hypodermal seam syncytium. Modified from Oren-Suissa *et al.* (2010); se, seam cells; c, cell body. (C) Cartoon summarizing the different stages in PVD regeneration following injury. Two-photon dendrotomy (see *Materials and Methods*) of the primary process (red arrowhead) leads to dynamic changes in the PVD arbor; loss of branch self-avoidance and growth is followed by primary branch fusion (blue arrowhead), menorah–menorah fusion (magenta bracket), or both. There is an additional phase of dynamic growth (asterisk) and pruning (black arrow), leading to arbor refinement. When the branches fail to fuse, the distal end undergoes degeneration. FF?, fusion family unidentified fusogen.

were anesthetized with 0.1% tricaine and 0.01% tetramisol in M9 solution (Kirby *et al.* 1990; McCarter *et al.* 1997, 1999). Animals were analyzed by Nomarski optics and fluorescence microscopy, using a Zeiss laser scanning microscope (LSM) 510 META confocal (Zeiss [Carl Zeiss], Thornwood, NY), the Zeiss LSM 700 confocal or Nikon eclipse Ti inverted microscope (Nikon, Carden City, NY) equipped with Yokogawa CSU-X1 spinning disk (Yokogawa, Tokyo, Japan) and a sCMOS (Andor, Belfast, UK) camera. Z-stacks were taken with PlanApochromat 60 × oil NA = 1.4 objective using the spinning disk confocal (SDC) or 63 × NA = 1.4 objective using the LSM. When using the sCMOS (Andor) camera z-stacks were taken with ~0.35 μm z-step. When the LSM 510 meta was used, z-step was ~0.8 μm. Image acquisition was done using Andor iQ or Metamorph software (Molecular Devices, Sunnyvale, CA) when using the SDC, and Zen software when using the LSM 510 meta microscope or Zeiss LSM 700. Multidimensional data were reconstructed as projections using the ImageJ and Metamorph softwares. Figures

were prepared using ImageJ, Adobe Photoshop CS5, and Adobe Illustrator CS6.

Quantifying PVD branching phenotypes and statistics

We defined primary branch fusion as reconnection of the distal and proximal primary branches via fusion, following injury. We verified continuity by analyzing GFP-signal continuity using confocal microscopy and live imaging. In addition, we used a photoconvertible Kaede cytoplasmic reporter expressed in the PVD to validate fusion. We define menorah–menorah fusion as connections via fusion between high order branches in injured animals. Menorah–menorah fusion was never observed in noninjured animals.

Quantification was done as previously described (Oren-Suissa *et al.* 2010). Using confocal microscopy, at least five sequential z-series pictures were taken from each worm. Each z-section was analyzed separately. The results from each worm were normalized to a longitudinal length of 100 μm in all relevant experiments. Significant differences between

mutants and wild-type were determined by the two-tailed unpaired *t*-test, the nonparametric Mann–Whitney test, or Fischer's exact test. For each group, we observed >20 additional animals that were not recorded by *z*-series on the confocal microscope and that showed similar phenotypes.

Laser surgery

Microsurgery was done using the LSM 510 META and a tunable multiphoton Chameleon Ultra Ti-Sapphire laser system (Coherent, Santa Clara, CA), that produces 200-fs short pulses with a repetition rate of 113 MHz and 5 nJ energy at a wavelength of 820 nm. Next, 0.5–2 μm^2 selected rectangular regions of interest of GFP-labeled PVD neurons were cut and successful surgery was confirmed by visualizing targets immediately after exposure. We evaluated the ability of severed neurons to reconnect by analyzing *z*-stack images of GFP-labeled branches. Dendrotomy was performed on the primary longitudinal process, and the morphological changes were followed for 2–72 hr after the surgery. Imaging before and after surgery was done as described above, using the 488-nm line of the Argon laser of the LSM microscope or using the SDC system. After surgery, animals were recovered to an agar plate and remounted 5–72 hr after surgery. Recovered worms were analyzed for regeneration, fusion between processes, and ectopic sprouting. At least 10 individuals were observed for each experiment. For all worms, the primary dendrite was injured anterior to cell body. Animals were imaged and a *z*-stack was collected immediately after injury to confirm a successful injury.

Photoactivation using Kaede

To verify that dendrites fuse as a response to injury, we used the photoconvertible protein Kaede driven by a PVD-specific promoter *ser-2prom3* (Yip and Heiman 2016). A PVD primary dendrite of *ser-2prom3*::*Kaede*-expressing animals was dendrotomized, animals were recovered for 23 hr, and the dendrite reconnection to its stump was assessed by Kaede photoconversion (Kravtsov *et al.* 2016). The green Kaede form in the PVD cell body was irreversibly photoconverted to the red Kaede form using a 405-nm laser with the Mosaic system (Andor) on the Nikon eclipse Ti inverted microscope. Following photoconversion of the Kaede in the cell body, we followed spreading to the dendritic branches for 1 and 60 min postphotoconversion. Red Kaede form, though diluted while spreading through the dendritic tree, can be observed beyond the reconnection site of injury in the distal part of the primary and higher ordered dendritic branches. When the dendrites failed to reconnect or immediately after dendrotomy, the photoconverted Kaede did not cross the site of injury, revealing that spreading of red Kaede is a reliable tool to confirm rejoining of severed dendrites.

Data availability

Strains are available upon request. The authors state that all data necessary for confirming the conclusions presented in the article are represented fully within the article.

Results

Dissection of dendritic regeneration in C. elegans mechanosensory neurons

The regenerative ability of axons following injury has been previously described in vertebrates and invertebrates (Cajal 1899; Hoy *et al.* 1967; Devor 1976; Bradbury *et al.* 2002; Fernandez-Gonzalez *et al.* 2002; Giordano-Santini *et al.* 2016). The morphological and molecular changes that occur following dendritic severing remain mostly unexplored (Standler and Bernstein 1982; Oren-Suissa and Podbilewicz 2010; Oren-Suissa *et al.* 2010; Stone *et al.* 2010, 2014; Nawabi *et al.* 2012; Song *et al.* 2012; Rao *et al.* 2016; Tao *et al.* 2016). To study the process of regeneration of the PVD dendrites following injury, we performed dendrotomy of arborized neurites using a femtosecond laser (Yanik *et al.* 2004; Bourgeois and Ben-Yakar 2007; Wu *et al.* 2007; Ghosh-Roy and Chisholm 2010). We found that the fate of the dendritic tree relies upon the ability of its branches to reconnect via fusion following injury. Failure to rejoin the two parts of the severed primary dendrite results in degeneration of the distal part and, in some cases, a complete degeneration without regrowth of the dendritic tree. Thus, we defined a successful regeneration event as a process in which the severed branch was able to reconnect with its target (Hilliard 2009). Temporal analysis of PVD dendrite dynamics following injury revealed several overlapping steps in arbor regeneration (Figure 1C).

Dendrotomy brings loss of self-avoidance

The dendritic architecture of the PVDs is maintained by a contact-dependent self-avoidance mechanism. The tertiary branches withdraw upon contact of a neighboring branch, maintaining the menorah architecture (Smith *et al.* 2010, 2012; Yip and Heiman 2016). To test whether self-avoidance is maintained after injury, we explored the spatial dynamics of regenerating dendrites. Two hours after injury, we observed tertiary branches from neighboring menorahs that contacted each other and extended far from their initial location, resulting in a structure of overlapping menorahs (Figure 2). Some of these overlaps extended and occurred between menorahs originating from both sides of the lesion (Figure 2B, brackets and Supplemental Material, File S1 and File S2). These overlapping structures persisted even 46 hr after the injury (Figure S1 in File S12).

Dendrotomy at earlier stages, such as the L3 stage, showed similar results; animals exhibited loss of avoidance mechanisms and branch overlap (data not shown). These results suggest that, upon injury, the avoidance mechanisms are lost, making it more likely that a new connection will form to compensate for the injury.

Following injury dendrites regenerate and reconnect via primary branch fusion

PVD dendrites showed robust regeneration when severed at the L4 stage. We found that severed primary dendrites grew
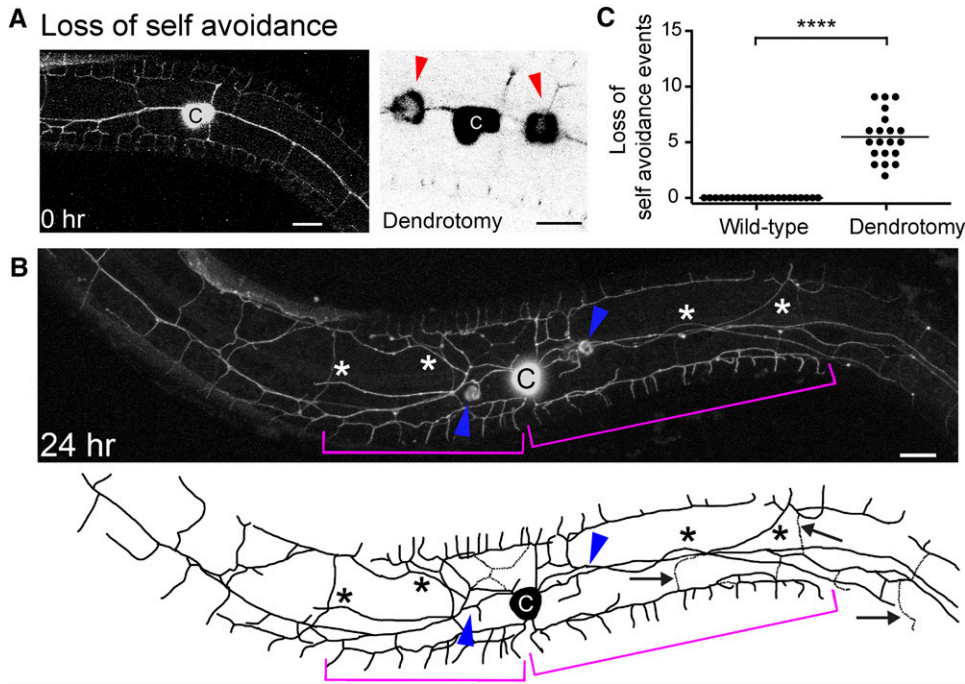
Figure 2 Dendritic injury induces loss of self-avoidance between adjacent menorahs. (A) Wild-type animal before dendrotomy (left panel) and two laser-induced injuries of primary branches, right panel. Red arrowheads mark injury sites. (B) Confocal projection and a schematic tracing of the same animal 24-hr postsurgery. Asterisks mark ectopic branching. Magenta brackets, giant menorahs. Blue arrowheads, primary branch fusion. Black arrows, secondary stem pruning and arbor simplification. (C) Quantitation of the number of loss of self-avoidance events, in an area of 200 μm around the cell body. In wild-type animals, PVD dendrites avoid one another and were not observed to overlap. Statistics were calculated using the nonparametric Mann–Whitney test. ****$P < 0.0001$. Wild-type animals, $n = 20$. Injured animals, $n = 21$. Horizontal line is the average. Bar, 10 μm. c, cell body.

toward each other (File S1 and File S2), and in 40% of the animals we observed reconnection of the distal end to the soma via fusion of the primary branches (Figure 3, B and C, "primary branch fusion," blue arrowhead). To directly measure reconnection by fusion, we used the photoconvertible reporter Kaede expressed in the PVD (Yip and Heiman 2016). The primary branch of *ser-2prom3*::*Kaede*-expressing animals was dendrotomized, and the animals were recovered for 23 hr before dendrite reconnection was assessed by Kaede photoconversion (Figure 3, D–H). Red Kaede was observed spreading from the cell body beyond the reconnected site of injury to the distal part of the primary and higher ordered dendritic branches. Thus, Kaede photoconversion and diffusion beyond the injury site demonstrate fusion between the severed primary dendrites. In animals where reconnection failed, photoconverted Kaede did not spread beyond the injury site (data not shown).

It was shown that, following axotomy of the PLM mechanosensory neuron, reconnection of the axon to the distal branch is dependent upon EFF-1, but not AFF-1 activity (Ghosh-Roy *et al.* 2010; Neumann *et al.* 2011, 2015). In contrast, we found that primary dendrotomies in *eff-1*-null mutants were repaired and regeneration via primary branch fusion occurred (Figure 3C). Thus, following primary branch microsurgery, the two ends grow toward each other, the tips meet, connect, and the integrity of the distal arbors is maintained.

Menorah–menorah fusion bypasses the severed primary dendrites

We have previously shown that during wild-type development, PVD and FLP terminal quaternary branches can autofuse with one another to maintain menorah structure and to

limit further growth (Oren-Suissa *et al.* 2010). To determine whether fusion of terminal dendrites is part of the regeneration process, we analyzed the overlapping branches after injury and found that most of the reconnections bypassed the injury site through menorah–menorah fusion, resulting in giant menorahs (Figure 4, magenta brackets). To judge the connectivity of the tertiary branches, we verified that the distal processes do not degenerate, and analyzed GFP-signal continuity using confocal microscopy and live imaging (Figure 4, File S1, File S2, and File S4). In addition, we used a photoconvertible Kaede cytoplasmic reporter expressed in the PVD (Yip and Heiman 2016) to demonstrate that the menorahs have fused to bypass the lesion site (Figure 4, E–G). We found that, in animals where menorah–menorah fusion took place, the distal fragment did not degenerate, regardless of primary–primary branch reconnection (Figure 4H; $n = 20$). Thus, terminal branch autofusion acts as a mechanism to bridge the gap between the PVD soma and the distal end to maintain connectivity and avoid degeneration.

Ectopic branching, pruning, and arbor simplification complete regeneration

In all animals assayed, failure to reconnect via fusion, following dendrotomy, resulted in degeneration of the distal end and took place within 12 hr in ~20% of the operated animals (Figure 5A, arrow, and File S3). Thus, the PVD fusion is essential for the survival of the elaborate tree structure following injury. There are several possible fusion outcomes following injury. The two severed primary branches could reconnect directly to one another via primary branch fusion. Alternatively, terminal branches from menorahs on both sides of the injury can reconnect via fusion ("menorah–menorah"
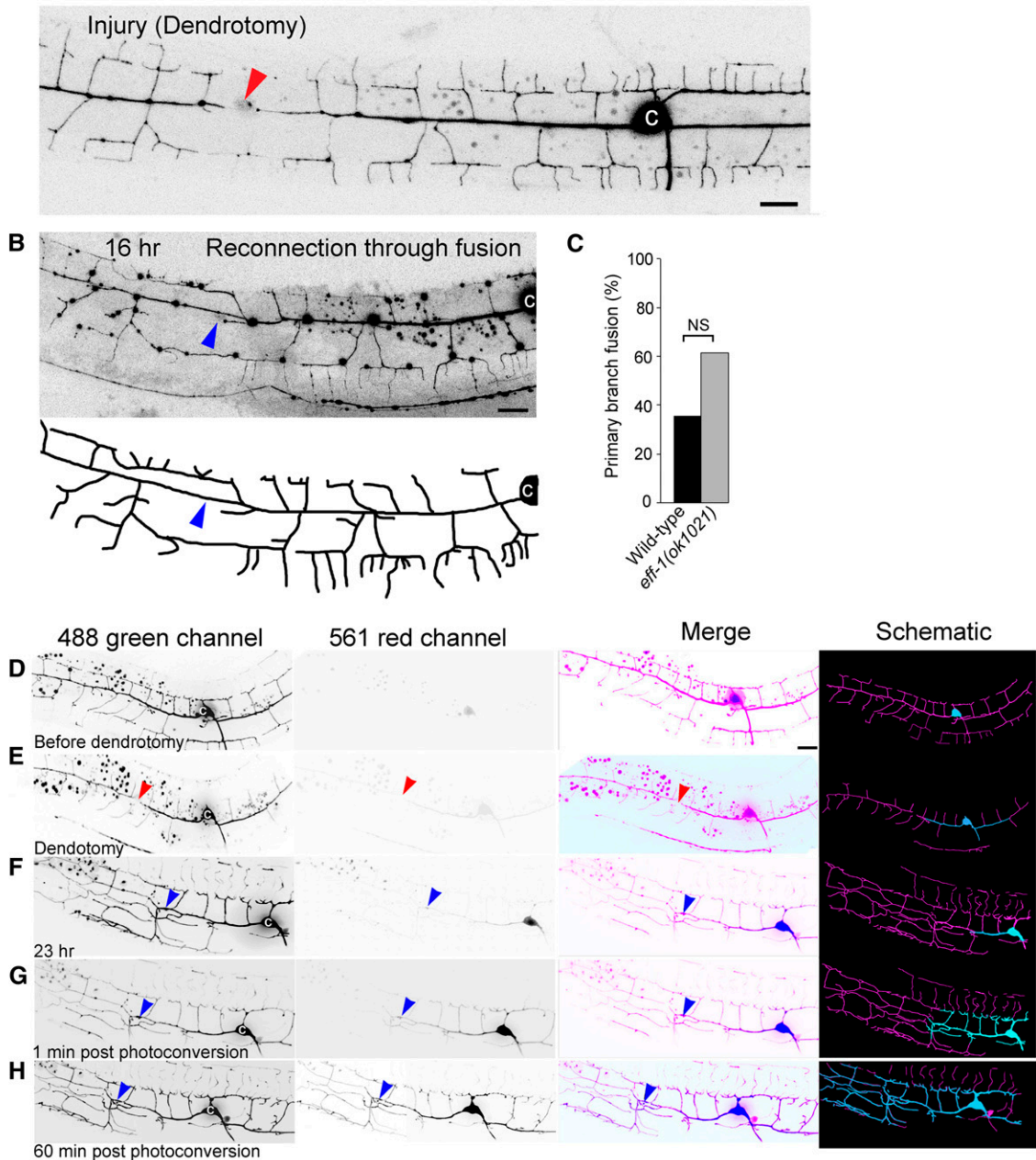
Figure 3 Primary branch fusion occurs following PVD dendrite injury. (A and B) Primary branch fusion following dendrotomy. L4 animal just after injury (red arrowhead in A) and 16-hr postsurgery (B). In (B), the severed distal and proximal ends of the primary branch reconnected (blue arrowhead). Bar, 10 μm. (C) Percentage of primary branch fusion during regeneration in wild-type (*n* = 14) and *eff-1(ok1021)* (*n* = 13) dendrotomized animals. Differences are not statistically significant (Fischer's exact test). (D-H) PVD dendrite reconnection confirmed by Kaede photoconversion. A PVD primary dendrite of *ser-2prom3*::*Kaede*-expressing animals was dendrotomized, the animal was recovered for 23 hr, and the dendrite reconnection to its stump was assessed by Kaede photoconversion. The green Kaede form in the PVD cell body was irreversibly photoconverted to the red Kaede form using a 405 nm laser with the Mosaic system, and its spreading throughout the dendritic branches was followed 1 and 60 min postphotoconversion. Panels left to right are confocal reconstructions of a wild-type dendrotomized animal in the 488 green channel, 561 red channel, two channels merged view, and a schematic representation of the merged view. (D) Confocal reconstructions of the animal before dendrotomy, (E) immediately post dendrotomy, (F) 23-hr postdendrotomy, (G) 1-min post-Kaede photoconversion, and (H) 60-min post-Kaede photoconversion. Red Kaede form (cyan in merged and schematic representations), though diluted when spreading through the dendritic tree, can be observed beyond the reconnected site of injury in the distal part of the primary and higher ordered dendritic branches. Red arrowhead, site of injury; blue arrowhead, site of primary branch fusion. In the merged and schematic columns: magenta, green Kaede and cyan, photoconverted red Kaede. c, PVD cell body; NS, not significant.
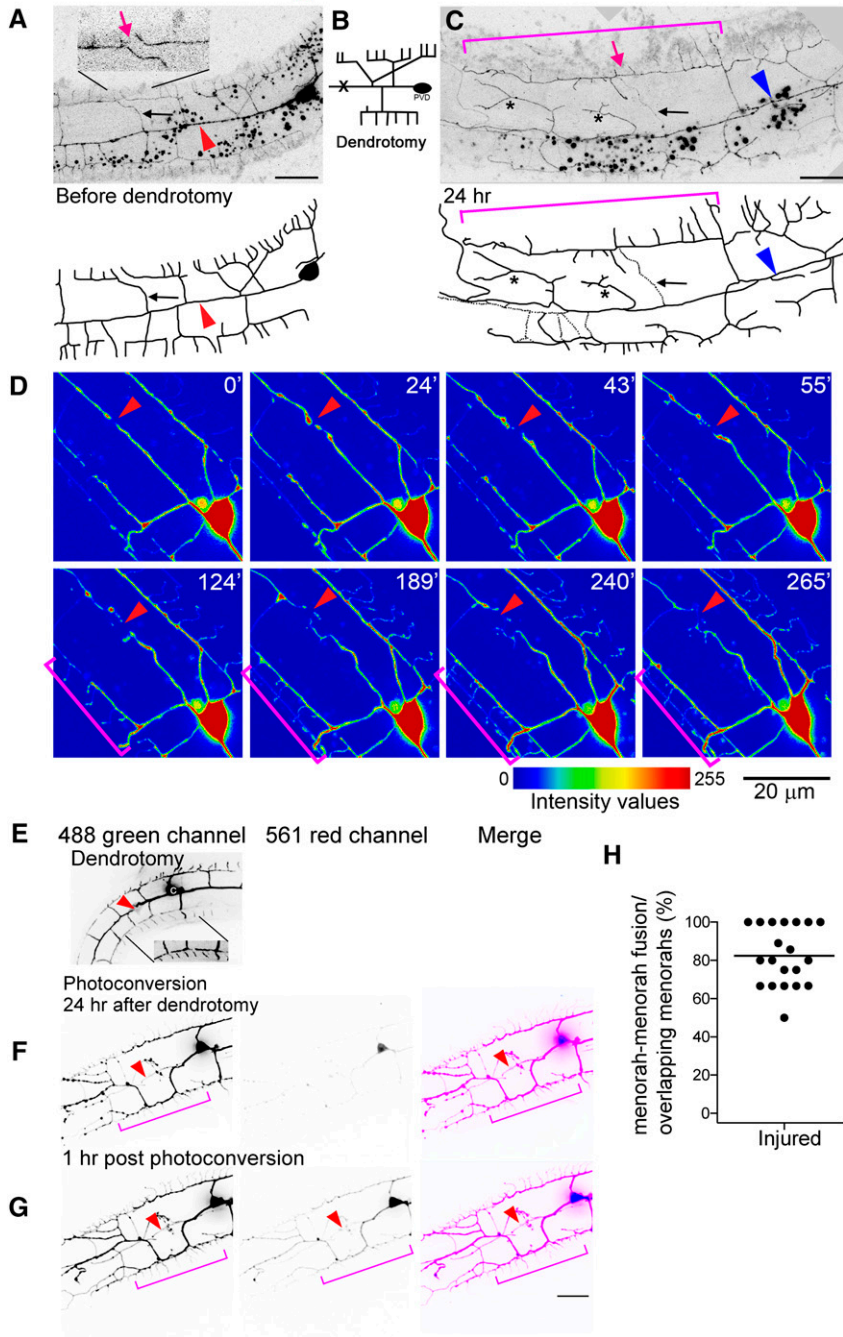
Figure 4 Menorah–menorah fusion bypasses the injury site and ensures dendrite continuity. (A–C) Dendrotomy of an L4 animal resulted in menorah–menorah fusion. Bar, 10 μm. (A) Just prior to the injury, separated menorahs can be seen (magenta arrow in inset). Red arrowhead points to the lesion site. (B) Schematic showing the site of injury (marked with an X). (C) Formation of giant menorahs (magenta bracket) and ectopic branching (asterisks) within 24 hr. Magenta arrow points to the site of loss of self-avoidance. Blue arrowhead points to the site of primary branch fusion. Pruning of secondary branches also occurs [black arrow, dotted lines, also marked in (A)]. (D) Intensity values view of images from a time-lapse movie of injured L4 wild-type worm (File S4). Time after injury is shown at the upper right corner in minutes. Red arrowheads point to injury site and pruning of branches. Brackets mark two menorahs from distal and proximal ends bypassing the break and contacting one another. (E–G) PVD menorah–menorah fusion confirmed by Kaede photoconversion. Bar, 10 μm. (H) The fraction of menorah–menorah fusion out of the number of loss of self-avoidance events (shown as percentage; horizontal line is the average). $n = 20$.

fusion). We also found that a third scenario existed, where primary branch fusion and menorah–menorah fusion both occurred. Analysis of these outcomes reveals that menorah fusion is the main mechanism used by PVD dendrites to reconnect following injury and remodeling (Figure 5B).

We analyzed the tree architecture following fusion and observed that the PVD dendrites appeared highly dynamic after injury, showing ectopic growth of terminal branches. These results suggested that growth is not restricted to a subset of branches and can occur throughout the neuron, allowing for massive regeneration (Figure 1C and Figure 2B,

asterisks). To verify that growth is stimulated specifically due to the dendrite injury and not because of laser damage, we examined mock-injured animals for PVD morphology changes. We injured animals near the PVDs, at the same focal plane, but without hitting any dendrites. PVD mock-operated animals showed normal growth with no excess sprouting or changes in the PVD morphology (data not shown). These results demonstrate that dendrite severing specifically induced terminal branch reconnection by fusion, ectopic branching, and regeneration (Figure 1C and File S1 and File S2).
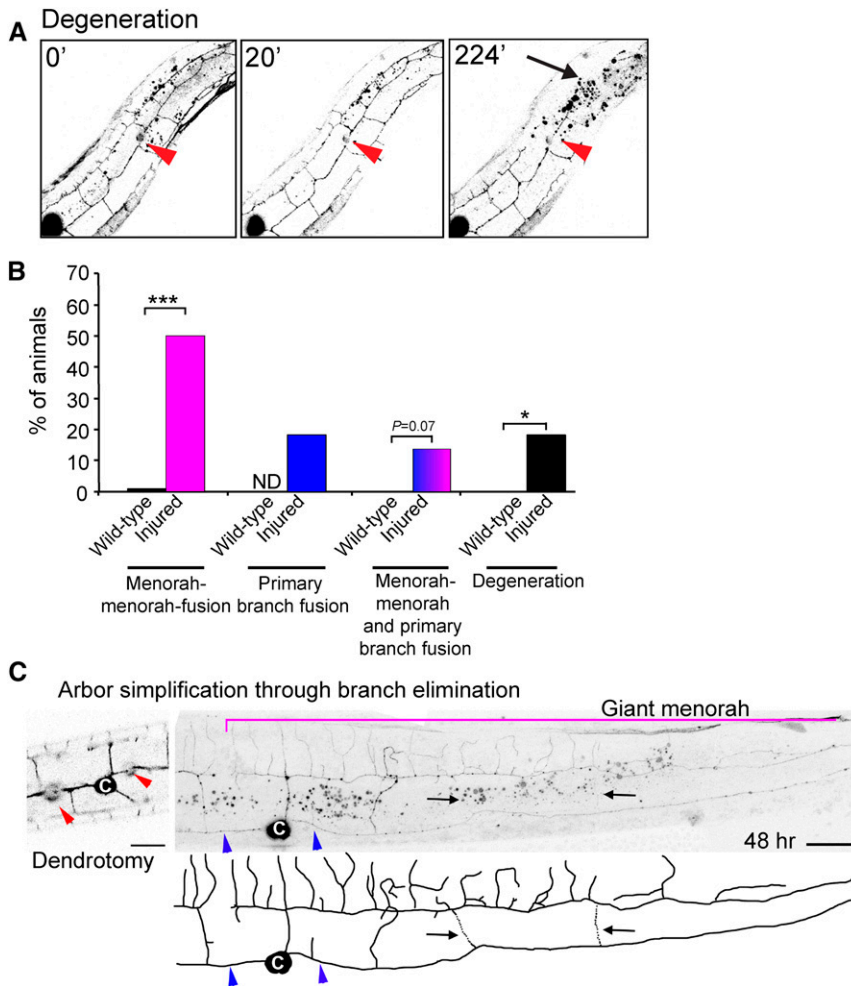
Figure 5 The dynamic pathway of PVD regeneration after injury. (A) Live imaging of an injured young-adult animal in which reconnection was unsuccessful, and degeneration of the distal arbor occurred. Time after injury is indicated in minutes. Red arrowhead, site of injury. Arrow, degenerating arbor. Images are taken from File S3. Posterior is up and dorsal is left. (B) Quantification of PVD postinjury outcomes displayed color coded as magenta = menorah–menorah fusion, blue = primary–primary fusion, magenta and blue = menorah–menorah fusion and primary–primary fusion, and black = degeneration. Statistics were calculated using Fischer's exact test. ***$P < 0.001$, *$P < 0.05$. Wild-type $n = 28$, wild-type following injury $n = 22$. (C) Menorah fusion and secondary stem pruning are part of the regeneration process of the PVDs following dendrotomy. Dendrotomy of an L4 wild-type animal. Red arrowheads point to sites of laser surgery. 48-hr postsurgery, giant menorah can be seen (magenta bracket); arrows (and dotted lines in the schematic tracing) point to secondary branches undergoing trimming. Blue arrowheads mark primary branch fusion at the sites of dendrotomy. Bar, 10 μm. c, cell body; ND, not determined.

Interestingly, some of the distal secondary stems were eliminated following the reconnection, leaving just one or two secondary stems per giant menorah (Figure 4C and Figure 5C; black arrows). These dendritic rearrangements persisted even 48 hr after surgery, leading to simplification of the dendritic trees and leaving mainly giant menorahs. Thus, active elimination of excess branches occurs to recreate a pattern resembling wild-type PVD architecture. Analysis of time-lapse movies showed that excess branches were eliminated, and pruning occurred concomitantly with growth around the injury site (Figure 4D and File S4). Taken together, the PVD dendrites are able to successfully regenerate following dendrotomy, inducing dynamic remodeling by branch growth and elimination (Figure 1C).

EFF-1 is essential for pruning excess branches after dendrotomy

The central function of EFF-1 in PVD developmental arborization is in quality control trimming of excess and abnormal branches (Oren-Suissa *et al.* 2010). To determine whether EFF-1 acts in simplification following injury, we amputated primary dendrites in *eff-1* mutants and followed the repair process. We found that *eff-1* mutants maintained hyper-branched and disorganized menorahs and failed to simplify the dendritic tree following injury (Figure 6A). These phenotypes suggest that *eff-1* acts in branch retraction and simplification induced by severing of the primary branch. We were not able to determine whether *eff-1* participates in menorah–menorah fusion because the hyperbranched and severely disorganized arbors prevented us from identifying menorah fusion and additional ectopic sprouting (Figure 6, B and C). Since the injured *eff-1*(*ok1021*) mutant animals analyzed degenerated to the same extent as wild-type (Figure 6E), we conclude that *eff-1* is neither required for dendrite reconnection nor for degeneration. We propose that in injured *eff-1* mutants where primary branch fusion was not observed (Figure 3C), it is possible that reconnection occurred via menorah–menorah fusion. In contrast, both uncut and dendrotomized *eff-1* mutants showed no pruning, demonstrating that *eff-1* is required for branch simplification following dendrotomy (Figure 6D). In addition, cell-autonomous expression of EFF-1 in the PVD resulted in excess pruning (Oren-Suissa *et al.* 2010; Kravtsov *et al.* 2016). Thus, EFF-1 may act cell-autonomously to simplify excess sprouting following dendrotomy and is sufficient to trim branches and simplify arbors.
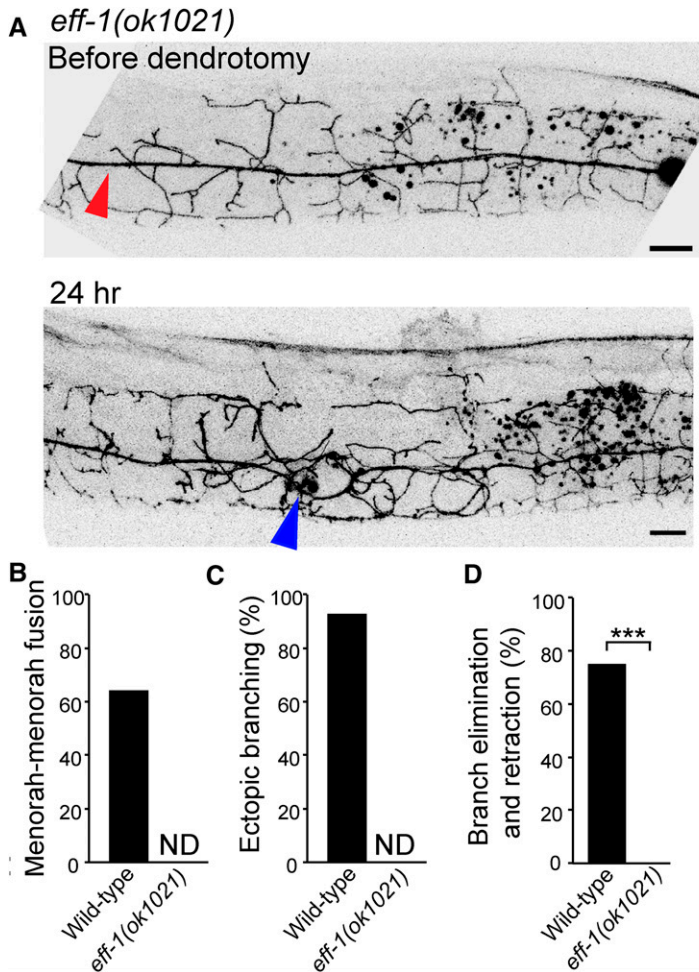
Figure 6 EFF-1 is essential for pruning excess branches after dendrotomy but not for primary branch fusion. (A) *eff-1*-null animal before and 24 hr after dendrotomy. There is a successful reconnection of the severed primary branch (arrowhead) and pruning failure (the arbor does not undergo simplification). Bar, 10 μm. (B–E) Dendrotomy-induced phenotypes in *eff-1(ok1021)* animals. Menorah–menorah fusion, percentage of animals that contained fused giant menorahs; ectopic branching, fraction of animals showing growth of additional processes; pruning, percentage of animals in which PVD underwent branch refinement after fusion. In *eff-1(ok1021)* mutants there is excess branching and disorganized branch structure (Oren-Suissa *et al.* 2010), thus we could not determine (ND) whether menorah–menorah connections and ectopic branching occurred. (D) Percentage of animals with branch elimination and retraction; ***$P < 0.001$, Fischer's exact test. *n* values: 14 and 13 animals for wild-type and *eff-1(ok1021)*, respectively. (E) Percentage of animals with degenerating distal end following dendrotomy in wild-type ($n = 14$) and *eff-1(ok1021)* ($n = 13$) animals. Differences are not statistically significant (Fischer's exact test). ND, not determined; NS, not significant.

AFF-1 is required to bypass cut dendrites via menorah–menorah fusion

Since the *C. elegans* known fusogens, EFF-1 and AFF-1, are essential and sufficient to fuse cells in *C. elegans* and heterologous cells in culture (Mohler *et al.* 2002; Shemer *et al.* 2004; Podbilewicz *et al.* 2006; Sapir *et al.* 2007; Avinoam *et al.* 2011), we hypothesized that they may be required to regenerate broken neurites by homotypic fusion. Because EFF-1 prunes dendrites by branch retraction (Oren-Suissa *et al.* 2010; Kravtsov *et al.* 2016), we decided to determine a possible role for *aff-1* following dendrotomy by asking whether menorah–menorah fusion occurs in *aff-1* injured-mutants. We found that while dendrite development was normal in *aff-1* mutants (Figure 7A), most of the reconnections were between the regrowing primary dendrite and its distal fragment following dendrotomy, rather than through menorah fusion as in wild-type animals (Figure 7E). This observation suggests a fusogenic function for AFF-1 in terminal branch fusion. In *aff-1* mutant animals, we found some exceptions in which some menorahs overlapped, but we did not observe fusion between menorahs followed by secondary stem degeneration (Figure 5C). In dendrotomized *aff-1* animals, failure to rejoin the dendritic trees resulted in degeneration of the distal part of the arbor (Figure 7, A and D). Thus, while *aff-1* has no apparent role in normal PVD arborization, it is required for terminal branch fusion following dendrotomy. Due to the subviability of *eff-1aff-1* double mutants (Sapir *et al.* 2007), we were unable to test whether there is redundancy between these genes in primary branch fusion. It is conceivable that there is redundancy in the fusion machinery that fixes broken neurites or that an unidentified fusogen is required for postembryonic primary dendrite auto-fusion after microsurgery.

AFF-1-mediated membrane fusion of terminal branches emerges as the main mechanism by which dendritic repair occurs in *C. elegans*. Using an *aff-1promoter*::GFP fusion and a fosmid-based AFF-1::GFP translational fusion, we did not detect *aff-1* expression in the PVD either before or after dendrotomy. Furthermore, PVD-expressing *des-2p*::AFF-1 was not able to rescue the fusion failure phenotype (Figure 7, D and E and Table 1). To determine whether AFF-1 acts extrinsically to the PVD to reconnect dendrites, we attempted to rescue fusion in *aff-1* mutants using expression of *grd-10p*::AFF-1 in the epithelial seam cells. This reduced degeneration to wild-type levels (Figure 7, B–D) and increased primary branch fusion (Figure 7E), but had little or no effect on menorah–menorah fusion (Figure 7E). These results suggest that AFF-1 functions cell nonautonomously for dendrite
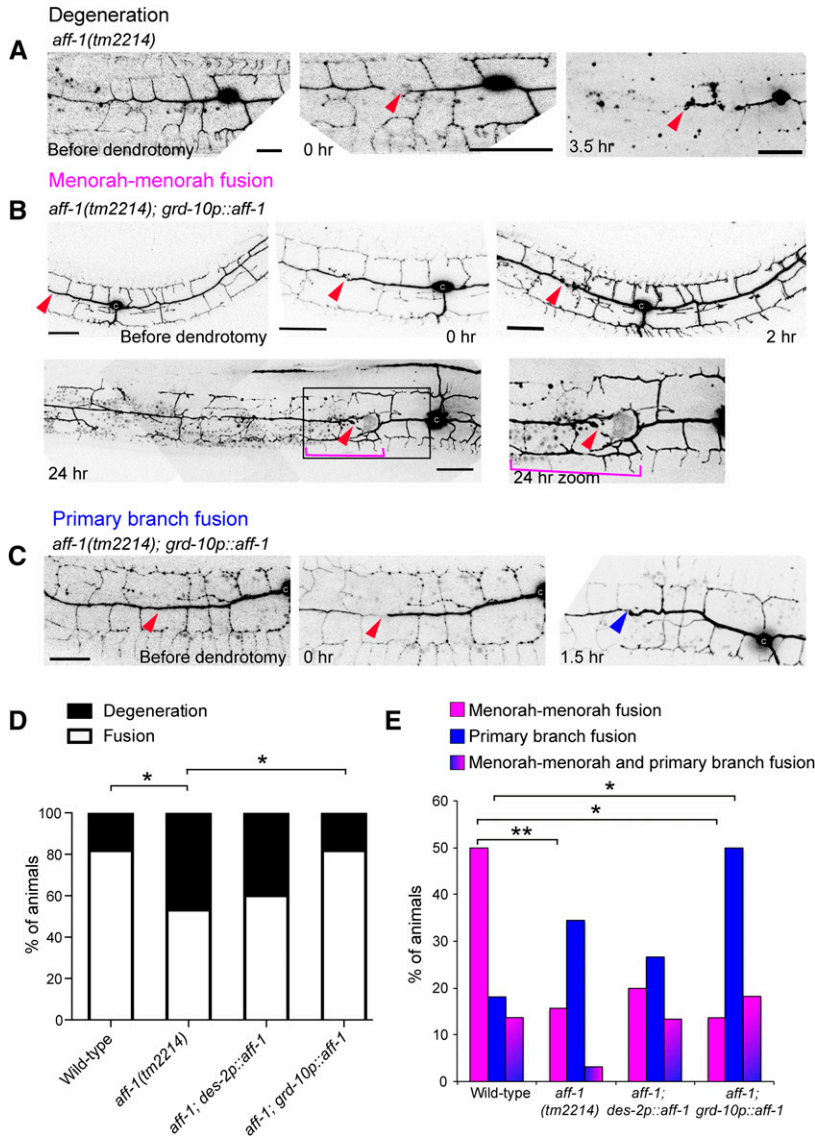
Figure 7 *aff-1* dendritic reconnection patterns are rescued cell nonautonomously. (A) Dendrite regeneration following PVD nanosurgery in *aff-1*(*tm2214*) mutant animal. PVD is shown before and after nanosurgery (*t* = 0 and 3.5 hr). In noninjured *aff-1* mutant animals, PVD branching pattern is unaffected. After injury, fusion does not occur and the distal processes undergo degeneration (*t* = 3.5 hr). (B) Dendrite regeneration following PVD nanosurgery in *aff-1*(*tm2214*); *grd-10p*::*aff-1* animals. PVD is shown before and after nanosurgery (*t* = 0, 2, and 24 hr). PVD reconnection occurred through fused menorahs (magenta bracket). Red arrowhead marks site of injury. Primary branches did not fuse (red arrowhead). (C) Dendrite regeneration following PVD nanosurgery in *aff-1*(*tm2214*); *grd-10p*::*aff-1* animals. PVD is shown before and after nanosurgery (*t* = 0 and 1.5 hr). PVD reconnection occurred through primary fusion (blue arrowhead). (D) Quantification of the fusion *vs.* degeneration outcomes in wild-type, *aff-1* mutant animals, and *aff-1* mutant with tissue-specific *aff-1* expression (*des-2* for PVD and *grd-10* for seam cells). Statistics were calculated using Fischer's exact test. *P < 0.05. (E) PVD postinjury outcomes displayed in color-coded bar graphs as magenta = menorah–menorah fusion, blue = primary–primary fusion, magenta and blue = menorah–menorah fusion and primary–primary fusion, and black = degeneration. Wild-type *n* = 22, *aff-1*(*tm2214*) *n* = 32, *aff-1*(*tm2214*);*des-2*::*aff-1* *n* = 15, and *aff-1*(*tm2214*); *grd-10p*::*aff-1* *n* = 22. **P < 0.01, *P < 0.05. Dendrotomy site = red arrowhead, fused menorah = magenta bracket, and primary fusion = blue arrowhead. Bar, 20 μm.

repair, but AFF-1 rescues primary dendrite fusion rather than menorah–menorah fusion. A possible explanation for this result is that the source of AFF-1 in the seam cells is only < 1000 nm away from the primary dendrite, and this proximity may facilitate primary dendrite reconnection. Moreover, if EFF-1 is required in the PVD to interact heterotypically with AFF-1, there may be a higher concentration of EFF-1 at the injury site. Last, the machinery of engulfment

has been reported to act together with EFF-1 in the repair of injured PLM mechanosensory axons (Neumann *et al.* 2011, 2015). In summary, it is conceivable that reconnection of dendrites functions more efficiently at the injury site.

Expression of *dpy-7p*::*aff-1* from the hypodermis was toxic in *aff-1* heterozygous *aff-1*/+ animals, suggesting that only nonautonomous expression from epithelial seam cells is sufficient to improve the ability of the PVD to rejoin the branches

Table 1 PVD postinjury outcomes

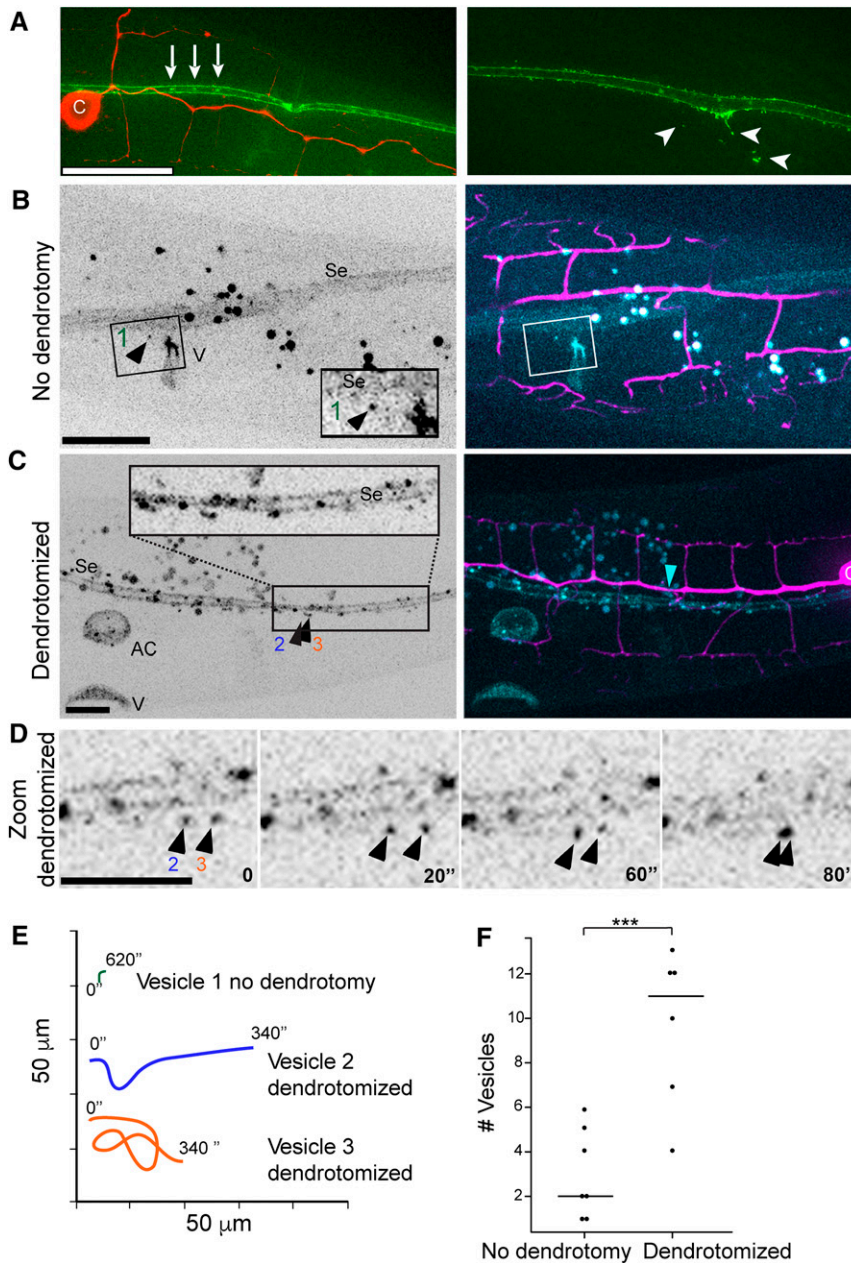| Genotype	Menorah–Menorah Fusion, %	Primary Branch Fusion, %	Menorah–Menorah and Primary Fusion, %	Degeneration, %	*n*
Wild-type	50	18.2	13.6	18.2	22
aff-1(*tm2214*)	15.6, *P = 0.01	34.4	3.1	46.9, *P = 0.04	32
aff-1(*tm2214*); *des-2p*::*aff-1*	20	26.7	13.3	40	15
aff-1(*tm2214*); *grd-10p*::*aff-1*	13.6, *P = 0.02	50, *P = 0.05	18.2	18.2, *P = 0.04, compared with *aff-1* mutant	22

Statistics calculated using Fischer's exact test.

Figure 8 AFF-1::GFP protein dynamics during PVD dendrite regeneration. (A) Superresolution structured illumination microscopy image of aligned *AFF-1::GFP* (green) vesicles in the seam cells (left, white arrows) and *AFF-1::GFP* extracellular vesicles derived from the seam cells (right, white arrowheads) in intact wild-type animals. c, cell body. PVD is labeled in red. (B) Spinning disk confocal images of *AFF-1::GFP* expression inside and outside the seam cells (Se), and in the vulva (V) of an intact L4 animal (left). *AFF-1::GFP* (cyan) expression in the seam cells and in vesicles near the seam cells is shown in a two channels merged image (right, PVD in magenta; File S5). Inset shows magnification of a single *AFF-1::GFP* vesicle near the seam cells (left, black arrowhead, numbered 1; File S6). (C) *AFF-1::GFP* expression inside and outside the seam cells (Se), in the anchor cell (AC), and in the vulva (V) of a reconnected PVD L4 animal (left) is shown 2-hr postdendrotomy in a spinning disk confocal image. *AFF-1::GFP* is expressed in vesicles inside and outside of the seam cells, in the anchor cell (AC) and in VulA ring (see File S7; right, blue arrowhead, site of reconnection). Inset shows magnification of area with multiple vesicles, two are labeled (2 and 3) and shown in (D and E). (D) Two *AFF-1::GFP* vesicles, numbered 2 and 3, are moving near the seam cells in a PVD dendrotomized animal. Four time points are shown (0, 20, 60, and 80 sec; File S8). (E) Vesicle dynamics (1, 2, and 3) is demonstrated in a color-coded graph during 340 sec for vesicles 2 and 3 and 620 sec for vesicle number 1. The plot illustrates vast differences between *AFF-1::GFP* vesicle movements in animals with an intact PVD *vs.* *AFF-1::GFP* vesicles in PVD dendrotomized animals (File S6 and File S8). (F) Dot plot of the number of *AFF-1::GFP* vesicles outside *aff-1*-expressing cells in animals with intact PVD *vs.* in animals with dendrotomized PVD. The graph demonstrates statistical significant difference between the mean number of *aff-1::GFP* vesicles outside *aff-1*-expressing organs such as seam cells, vulva, anchor cells, and the uterus. ***$P = 0.001$, statistics were calculated using the nonparametric Mann–Whitney test.

by fusion (Figure S2 in File S12). The cell nonautonomous activity of AFF-1 in PVD regeneration by auto-fusion was unexpected since for cell–cell fusion, AFF-1 is required in both fusing plasma membranes (Avinoam *et al.* 2011).

AFF-1-containing extracellular vesicles (EVs) may repair the PVD by fusing with it

To determine AFF-1 expression and localization before and after dendrotomy, we imaged AFF-1 in worms expressing mCherry in the PVD, using a 30-kb fosmid-based GFP reporter (Sarov *et al.* 2006). We could not detect AFF-1 in the PVD at any stage during development or following dendrotomy. Instead, AFF-1 is strongly expressed on the plasma membrane, filopodia, and internal puncta in the epidermal lateral seam cells. This was expected since the seam cells

fuse homotypically between the L4 and adult molt via AFF-1-mediated fusion (Sapir *et al.* 2007). Using structured illumination microscopy, we found extracellular puncta containing AFF-1::GFP that were apparently derived from the seam cells (Figure 8A, arrowheads). Using live SDC microscopy, we found that the vesicles containing AFF-1::GFP were observed outside the seam cells in control animals that were not dendrotomized (Figure 8B and File S5, File S6, and File S9). Following dendrotomy, the AFF-1::GFP signal in the seam cells was brighter (Figure 8C) and there was a fivefold increase in the mobility and number of EVs (Figure 8, D–F, File S7, File S8, File S10, and File S11). Thus, taken together, our results show that AFF-1 regenerates severed PVD dendrites in a surprisingly cell nonautonomous way from the seam cells.
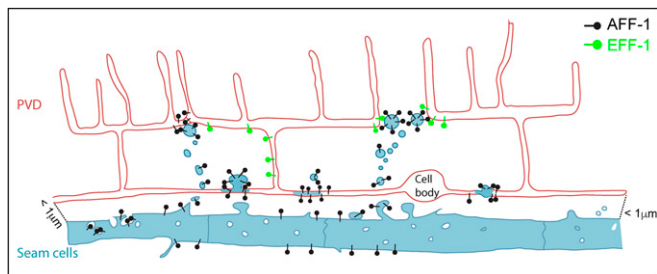
Figure 9 Model of AFF-1-mediated repair via extracellular vesicle-cell fusion. PVD (red) is in close proximity to the epithelial seam cells (blue). AFF-1 (black pins) is expressed in seam cells and additional tissues, but not in the PVD. Upon injury, AFF-1-containing extracellular vesicles (EVs) are highly released from the seam cells. Some of these EVs reach the PVD and promote fusion of severed dendrites. EFF-1 (green pins) is expressed in the PVD but it does not act to fuse severed dendrites on its own. Instead, it may collaborate with AFF-1-EVs. We propose that menorah–menorah fusion is mediated by AFF-1-EVs that merge with the structurally compatible EFF-1 expressed in the PVD. EFF-1-coated pseudotyped viruses can fuse with cells expressing AFF-1 on their surface and vice versa (Avinoam *et al.* 2011).

Discussion

Hypothesis: AFF-1-EVs merge injured neurons from without

Cell–cell fusion from within occurs when a fusogenic protein (*e.g.*, a viral fusion protein following infection) or an endogenous cellular fusion protein (*e.g.*, EFF-1) is expressed intrinsically in cellular compartments, including the plasma membrane (Podbilewicz and Chernomordik 2005; Oren-Suissa and Podbilewicz 2010). Fusion from without occurs when a viral particle fuses target cells without infecting them (Bratt and Gallaher 1969; White *et al.* 1981; Clavel and Charneau 1994; Duelli and Lazebnik 2007). Here, we discovered an example of fusion from without during neuronal regeneration. We propose that epidermal seam cells shed EVs that travel 1000 nm or less to reach the PVD severed dendrites and the menorahs. These vesicles contain AFF-1 and can fuse dendrites from without (Figure 9).

AFF-1-containing vesicles derived from the lateral epidermal seam cells mediate fusion of severed dendrites and menorah auto-fusion to bypass the injury and to maintain dendritic tree structure and function. EVs (microvesicles, exosomes, and ectosomes) from different subcellular and tissue origins have been proposed as vehicles for cell–cell communication during normal physiology, participate in the immune response, control coagulation, and promote metastatic cancer (Tkach and Thery 2016). These EVs have been shown to exist in bacteria, archea, protists, plants, fungi, and animals (Beveridge 1999; Liegeois *et al.* 2006; Miyado *et al.* 2008; Kwon *et al.* 2014; Hyenne *et al.* 2015). In *C. elegans*, EVs derived from ciliated neurons affect mating behavior and communication between animals (Wang *et al.* 2014). Signaling EVs derived from the sperm activate oogenesis and ovarian muscle contraction (Kosinski *et al.* 2005). EVs also participate in engulfment of dead cells (Mapes *et al.* 2012) and morphogenesis of the embryo (Wehman *et al.* 2011).

EVs are probably universal but diverge in size, shape, and place of origin. They contain lipid bilayers, transmembrane proteins, and nucleic acids. One of the characteristics of these EVs is their ability to fuse to target cells and deliver RNAs, plasmids, toxins, and signaling molecules. However, the fusion proteins necessary to deliver and merge the diverse EVs have not been identified and characterized in any system. Mammalian cells transfected with *C. elegans* AFF-1 produce EVs that have been biochemically and ultrastructurally characterized (Avinoam *et al.* 2011; Fridman 2012). Moreover, AFF-1-containing vesicles and pseudotyped particles are able to fuse to mammalian cells expressing EFF-1 or AFF-1. Thus, AFF-1 can mediate fusion of EVs to cells expressing EFF-1 on the plasma membrane in a tissue culture system (Avinoam *et al.* 2011; Fridman 2012). Recently, pseudotyped particles and vesicles containing a sperm protein from plants that is structurally similar to EFF-1 were shown to mediate fusion to cells expressing EFF-1 (Valansi *et al.* 2017). Here, we provide the initial evidence for a proposed mechanism that can fuse EVs to target neuronal cells *in vivo*. Surprisingly, these EVs can cause auto-fusion from without mediated by AFF-1 transmembrane fusion protein on their surface. Moreover, in our working model, these AFF-1-EVs derived from the *C. elegans* lateral epithelia can fuse neurons *in vivo*, thus directly promoting regeneration (Figure 9).

Neurodevelopmental genetic stages in dendrite repair after injury

The mechanism of PVD dendritic regeneration can be divided into five stages: (1) reattachment at site of injury, (2) loss of self-avoidance between adjacent menorahs, (3) menorah–menorah fusion to bypass lesions, (4) sprouting of compensatory branches, and (5) pruning of excess branches (Figure 1C).

The interplay between two effector fusogens revealed a genetic pathway that links membrane remodeling during development and following neuronal injury. Here, we focused on two cellular stages: extrinsic stage (3) AFF-1-mediated menorah–menorah fusion from without and intrinsic stage (5) EFF-1-mediated trimming of excess branches from within (Figure 1C and Figure 9).

AFF-1 merges terminal branches to bypass broken dendrites

Axonal fusion after injury is crucial for reestablishing synaptic contacts, to prevent degeneration, and for regaining neurological functionality (Hilliard 2009; Giordano-Santini *et al.* 2016). Although *eff-1* mutants failed to fuse broken axons (Ghosh-Roy *et al.* 2010), *eff-1* mutants succeed to merge injured dendrites. We tested the two known *C. elegans* fusogens, EFF-1 and AFF-1, as well as the EFF-1 paralog C26D10.7 (Mohler *et al.* 2002; Avinoam and Podbilewicz 2011) (M. Oren-Suissa and B. Podbilewicz, unpublished results). We found that terminal branch fusion following dendrotomy was significantly reduced in *aff-1* mutants compared to wild-type. However, none of these genes was independently required for primary dendrite fusion

following an injury, suggesting either redundancy or that yet another *C. elegans* fusogen awaits identification. Based on these observations, we conclude that *aff-1* is required to heal dendritic wounds, specifically via menorah–menorah fusion.

Our data support a model in which *aff-1* and *eff-1* expression is highly regulated in the PVD. In this working model, dendrotomy may initially repress EFF-1 surface expression allowing ectopic sprouting of terminal branches and loss of self-avoidance, culminating with AFF-1-mediated menorah–menorah fusion via a surprising cell nonautonomous mechanism of fusion from without (Figure 9).

Is auto-fusion an alternative pathway to repair severed neurons?

Fusion of severed axons occurs in invertebrates, for example in *Aplysia* (Bedi and Glanzman 2001), crayfish (Hoy *et al.* 1967), and *C. elegans* (Yanik *et al.* 2004; Ghosh-Roy and Chisholm 2010; Neumann *et al.* 2011, 2015), but rarely in vertebrates (Paltsyn *et al.* 2013; Li *et al.* 2016). Why is this the case and how can our study help us understand this? Invertebrates and vertebrates do have conserved pathways to regenerate injured branches via regrowth (Park *et al.* 2008; Yan *et al.* 2009; Ghosh-Roy and Chisholm 2010; Bradke *et al.* 2012; Yaniv *et al.* 2012; Mar *et al.* 2014; Stone *et al.* 2014; Ruschel *et al.* 2015; Rao *et al.* 2016; Tao *et al.* 2016). However, it appears that fusion of broken neurites or bypassing the injured site using fusion instead of rebuilding complex trees is a more energetically economical process. The use of EVs could be a useful strategy to stimulate repair of injured branches in the CNS of vertebrates that usually cannot regenerate.

Severed neurites can reconnect by suspending self-repulsion mechanisms

We have found that in *C. elegans* PVD, following dendrotomy, there is a transient loss of self-avoidance between tertiary branches that allows the reconnection by merging the menorahs and bypassing the site of injury, thus maintaining the dendritic trees. This is consistent with studies in leech embryos showing that laser microbeam severing of neurites of mechanosensory neurons result in that the detached branch stop being avoided by the rest of the cell. This is consistent with a mechanism that controls self-avoidance and that requires physical continuity between the neurites (Wang and Macagno 1998). In *C. elegans*, this mechanism appears to involve netrins (Smith *et al.* 2012). In contrast, in zebrafish, detached fragments continue to repel the parent arbor (Martin *et al.* 2010). Thus, in zebrafish and probably in other vertebrates, it is required to have a WD-like mechanism to remove fragments of sensory neurites before the process of regrowth can occur. It would be useful to find ways to induce merging of the severed neurites as occurs in some invertebrates.

Spinal cord injuries, experimental axotomies, surgical accidents, stroke, and diverse forms of neurodegeneration are all conditions that currently cannot be generally repaired (Devor 1976; Fernandez-Gonzalez *et al.* 2002; Moritz *et al.* 2008;

Ruschel *et al.* 2015; Li *et al.* 2016). Unveiling the mechanism of intrinsic *eff-1*-mediated dendritic simplification and extrinsic *aff-1*-mediated neuronal auto-fusion from without may pave the way for overcoming neurodegenerative diseases or brain injuries. In *C. elegans*, AFF-1-containing vesicles derived from epithelia appear to fuse dendrites, emerging as a potential effector that could repair broken neurons in heterologous systems.

Literature Cited

Aguirre-Chen, C., H. E. Bulow, and Z. Kaprielian, 2011 *C. elegans bicd-1*, homolog of the *Drosophila* dynein accessory factor *Bicaudal D*, regulates the branching of PVD sensory neuron dendrites. Development 138: 507–518.

Albeg, A., C. Smith, M. Chatzigeorgiou, D. G. Feitelson, D. H. Hall *et al.*, 2011 *C. elegans* multi-dendritic sensory neurons: morphology and function. Mol. Cell. Neurosci. 46: 308–317.

Avinoam, O., and B. Podbilewicz, 2011 Eukaryotic cell-cell fusion families. Curr. Top. Membr. 68: 209–234.

Avinoam, O., K. Fridman, C. Valansi, I. Abutbul, T. Zeev-Ben-Mordehai *et al.*, 2011 Conserved eukaryotic fusogens can fuse viral envelopes to cells. Science 332: 589–592.

Bedi, S. S., and D. L. Glanzman, 2001 Axonal rejoining inhibits injury-induced long-term changes in *Aplysia* sensory neurons *in vitro*. J. Neurosci. 21: 9667–9677.

Beveridge, T. J., 1999 Structures of gram-negative cell walls and their derived membrane vesicles. J. Bacteriol. 181: 4725–4733.

Bond, S. R., and C. C. Naus, 2012 RF-Cloning.org: an online tool for the design of restriction-free cloning projects. Nucleic Acids Res. 40: W209–W213.

Bourgeois, F., and A. Ben-Yakar, 2007 Femtosecond laser nano-axotomy properties and their effect on axonal recovery in *C. elegans*. Opt. Express 15: 8521–8531.

Bradbury, E. J., L. D. Moon, R. J. Popat, V. R. King, G. S. Bennett *et al.*, 2002 Chondroitinase ABC promotes functional recovery after spinal cord injury. Nature 416: 636–640.

Bradke, F., J. W. Fawcett, and M. E. Spira, 2012 Assembly of a new growth cone after axotomy: the precursor to axon regeneration. Nat. Rev. Neurosci. 13: 183–193.

Bratt, M. A., and W. R. Gallaher, 1969 Preliminary analysis of the requirements for fusion from within and fusion from without by Newcastle disease virus. Proc. Natl. Acad. Sci. USA 64: 536–543.

Brenner, S., 1974 The genetics of Caenorhabditis elegans. Genetics 77: 71–94.

Cajal, S. R., 1899 Histología del Sistema Nervioso del Hombre y de Los Vertebrados. Ministerio de Sanidad y Consumo, Madrid.

Chatzigeorgiou, M., and W. R. Schafer, 2011 Lateral facilitation between primary mechanosensory neurons controls nose touch perception in C. elegans. Neuron 70: 299–309.

Chatzigeorgiou, M., S. Yoo, J. D. Watson, W. H. Lee, W. C. Spencer et al., 2010 Specific roles for DEG/ENaC and TRP channels in touch and thermosensation in C. elegans nociceptors. Nat. Neurosci. 13: 861–868.

Chiorazzi, M., L. Rui, Y. Yang, M. Ceribelli, N. Tishbi et al., 2013 Related F-box proteins control cell death in Caenorhabditis elegans and human lymphoma. Proc. Natl. Acad. Sci. USA 110: 3943–3948.

Chisholm, A. D., H. Hutter, Y. Jin, and W. G. Wadsworth, 2016 The genetics of axon guidance and axon regeneration in Caenorhabditis elegans. Genetics 204: 849–882.

Clavel, F., and P. Charneau, 1994 Fusion from without directed by human immunodeficiency virus particles. J. Virol. 68: 1179–1185.

Coleman, M. P., and M. R. Freeman, 2010 Wallerian degeneration, Wld^S, and Nmnat. Annu. Rev. Neurosci. 33: 245–267.

Devor, M., 1976 Neuroplasticity in the rearrangement of olfactory tract fibers after neonatal transection in hamsters. J. Comp. Neurol. 166: 49–72.

Dong, X., H. Chiu, Y. J. Park, W. Zou, Y. Zou et al., 2016 Precise regulation of the guidance receptor DMA-1 by KPC-1/Furin instructs dendritic branching decisions. eLife. 5: e11008.

Duelli, D., and Y. Lazebnik, 2007 Cell-to-cell fusion as a link between viruses and cancer. Nat. Rev. Cancer 7: 968–976.

Edwards, T. J., and M. Hammarlund, 2014 Syndecan promotes axon regeneration by stabilizing growth cone migration. Cell Rep. 8: 272–283.

Fernandez-Gonzalez, A., A. R. La Spada, J. Treadaway, J. C. Higdon, B. S. Harris et al., 2002 Purkinje cell degeneration (pcd) phenotypes caused by mutations in the axotomy-induced gene, Nna1. Science 295: 1904–1906.

Fridman, K., 2012 Ultrastructure and function of AFF-1 and EFF-1 in membrane remodeling. M.Sc. Thesis, Technion - Israel Institute of Technology, Haifa, Israel.

Gabel, C. V., F. Antoine, C. F. Chuang, A. D. Samuel, and C. Chang, 2008 Distinct cellular and molecular mechanisms mediate initial axon development and adult-stage axon regeneration in C. elegans. Development 135: 1129–1136.

Gattegno, T., A. Mittal, C. Valansi, K. C. Nguyen, D. H. Hall et al., 2007 Genetic control of fusion pore expansion in the epidermis of Caenorhabditis elegans. Mol. Biol. Cell 18: 1153–1166.

Ghosh-Roy, A., and A. D. Chisholm, 2010 Caenorhabditis elegans: a new model organism for studies of axon regeneration. Dev. Dyn. 239: 1460–1464.

Ghosh-Roy, A., Z. Wu, A. Goncharov, Y. Jin, and A. D. Chisholm, 2010 Calcium and cyclic AMP promote axonal regeneration in Caenorhabditis elegans and require DLK-1 kinase. J. Neurosci. 30: 3175–3183.

Giordano-Santini, R., C. Linton, and M. A. Hilliard, 2016 Cell-cell fusion in the nervous system: alternative mechanisms of development, injury, and repair. Semin. Cell Dev. Biol. 60: 146–154.

Goodman, M. B., 2003 Sensation is painless. Trends Neurosci. 26: 643–645.

Halevi, S., J. McKay, M. Palfreyman, L. Yassin, M. Eshel et al., 2002 The C. elegans ric-3 gene is required for maturation of nicotinic acetylcholine receptors. EMBO J. 21: 1012–1020.

Hall, D. H., and M. Treinin, 2011 How does morphology relate to function in sensory arbors? Trends Neurosci. 34: 443–451.

Hall, G. F., and M. J. Cohen, 1988 Dendritic amputation redistributes sprouting evoked by axotomy in lamprey central neurons. J. Neurosci. 8: 3598–3606.

Hammarlund, M., and Y. Jin, 2014 Axon regeneration in C. elegans. Curr. Opin. Neurobiol. 27: 199–207.

Hammarlund, M., P. Nix, L. Hauth, E. M. Jorgensen, and M. Bastiani, 2009 Axon regeneration requires a conserved MAP kinase pathway. Science 323: 802–806.

Hilliard, M. A., 2009 Axonal degeneration and regeneration: a mechanistic tug-of-war. J. Neurochem. 108: 23–32.

Hoy, R. R., G. D. Bittner, and D. Kennedy, 1967 Regeneration in crustacean motoneurons: evidence for axonal fusion. Science 156: 251–252.

Hyenne, V., A. Apaydin, D. Rodriguez, C. Spiegelhalter, S. Hoff-Yoessle et al., 2015 RAL-1 controls multivesicular body biogenesis and exosome secretion. J. Cell Biol. 211: 27–37.

Kirby, C., M. Kusch, and K. Kemphues, 1990 Mutations in the par genes of Caenorhabditis elegans affect cytoplasmic reorganization during the first cell cycle. Dev. Biol. 142: 203–215.

Kosinski, M., K. McDonald, J. Schwartz, I. Yamamoto, and D. Greenstein, 2005 C. elegans sperm bud vesicles to deliver a meiotic maturation signal to distant oocytes. Development 132: 3357–3369.

Kravtsov, V., M. Oren-Suissa, and B. Podbilewicz, 2016 Cell fusion proteins can rejuvenate adult dendritic trees. bioRxiv. Available at: http://www.biorxiv.org/content/early/2016/07/07/062679.

Kwon, S. H., K. D. Liu, and K. E. Mostov, 2014 Intercellular transfer of GPRC5B via exosomes drives HGF-mediated outward growth. Curr. Biol. 24: 199–204.

Li, S., C. Yang, L. Zhang, X. Gao, X. Wang et al., 2016 Promoting axon regeneration in the adult CNS by modulation of the melanopsin/GPCR signaling. Proc. Natl. Acad. Sci. USA 113: 1937–1942.

Liang, X., X. Dong, D. G. Moerman, K. Shen, and X. Wang, 2015 Sarcomeres pattern proprioceptive sensory dendritic endings through UNC-52/Perlecan in C. elegans. Dev. Cell 33: 388–400.

Liegeois, S., A. Benedetto, J. M. Garnier, Y. Schwab, and M. Labouesse, 2006 The V0-ATPase mediates apical secretion of exosomes containing Hedgehog-related proteins in Caenorhabditis elegans. J. Cell Biol. 173: 949–961.

Maniar, T. A., M. Kaplan, G. J. Wang, K. Shen, L. Wei et al., 2012 UNC-33 (CRMP) and ankyrin organize microtubules and localize kinesin to polarize axon-dendrite sorting. Nat. Neurosci. 15: 48–56.

Mapes, J., Y. Z. Chen, A. Kim, S. Mitani, B. H. Kang et al., 2012 CED-1, CED-7, and TTR-52 regulate surface phosphatidylserine expression on apoptotic and phagocytic cells. Curr. Biol. 22: 1267–1275.

Mar, F. M., A. Bonni, and M. M. Sousa, 2014 Cell intrinsic control of axon regeneration. EMBO Rep. 15: 254–263.

Martin, S. M., G. S. O'Brien, C. Portera-Cailliau, and A. Sagasti, 2010 Wallerian degeneration of zebrafish trigeminal axons in the skin is required for regeneration and developmental pruning. Development 137: 3985–3994.

McCarter, J., B. Bartlett, T. Dang, and T. Schedl, 1997 Soma-germ cell interactions in Caenorhabditis elegans: multiple events of hermaphrodite germline development require the somatic sheath and spermathecal lineages. Dev. Biol. 181: 121–143.

McCarter, J., B. Bartlett, T. Dang, and T. Schedl, 1999 On the control of oocyte meiotic maturation and ovulation in Caenorhabditis elegans. Dev. Biol. 205: 111–128.

Mello, C., and A. Fire, 1995 DNA transformation, pp. 451–482 in *Methods in Cell Biology. Caenorhabditis Elegans: Model Biological Analysis of an Organism*, edited by H. F. Epstein, and D. C. Shakes. Academic Press, San Diego.

Miyado, K., K. Yoshida, K. Yamagata, K. Sakakibara, M. Okabe *et al.*, 2008 The fusing ability of sperm is bestowed by CD9-containing vesicles released from eggs in mice. Proc. Natl. Acad. Sci. USA 105: 12921–12926.

Mohler, W. A., G. Shemer, J. del Campo, C. Valansi, E. Opoku-Serebuoh *et al.*, 2002 The type I membrane protein EFF-1 is essential for developmental cell fusion in *C. elegans*. Dev. Cell 2: 355–362.

Moritz, C. T., S. I. Perlmutter, and E. E. Fetz, 2008 Direct control of paralysed muscles by cortical neurons. Nature 456: 639–642.

Nawabi, H., K. Zukor, and Z. He, 2012 No simpler than mammals: axon and dendrite regeneration in *Drosophila*. Genes Dev. 26: 1509–1514.

Neumann, B., K. C. Nguyen, D. H. Hall, A. Ben-Yakar, and M. A. Hilliard, 2011 Axonal regeneration proceeds through specific axonal fusion in transected *C. elegans* neurons. Dev. Dyn. 240: 1365–1372.

Neumann, B., S. Coakley, R. Giordano-Santini, C. Linton, E. S. Lee *et al.*, 2015 EFF-1-mediated regenerative axonal fusion requires components of the apoptotic pathway. Nature 517: 219–222.

Nix, P., M. Hammarlund, L. Hauth, M. Lachnit, E. M. Jorgensen *et al.*, 2014 Axon regeneration genes identified by RNAi screening in *C. elegans*. J. Neurosci. 34: 629–645.

Oren-Suissa, M., and B. Podbilewicz, 2010 Evolution of programmed cell fusion: common mechanisms and distinct functions. Dev. Dyn. 239: 1515–1528.

Oren-Suissa, M., D. Hall, M. Treinin, G. Shemer, and B. Podbilewicz, 2010 The fusogen EFF-1 controls sculpting of mechanosensory dendrites. Science 328: 1285–1288.

Paltsyn, A., S. Komissarova, I. Dubrovin, and A. Kubatiev, 2013 Increased cell fusion in cerebral cortex may contribute to poststroke regeneration. Stroke Res. Treat. 2013: 869327.

Park, K. K., K. Liu, Y. Hu, P. D. Smith, C. Wang *et al.*, 2008 Promoting axon regeneration in the adult CNS by modulation of the PTEN/mTOR pathway. Science 322: 963–966.

Petersen, L. K., and R. S. Stowers, 2011 A Gateway MultiSite recombination cloning toolkit. PLoS One 6: e24531.

Podbilewicz, B., 2014 Virus and cell fusion mechanisms. Annu. Rev. Cell Dev. Biol. 30: 111–139.

Podbilewicz, B., and L. V. Chernomordik, 2005 Cell fusion in development and disease, pp. 221–244 in *Protein-Lipids Interactions*, edited by L. K. Tamm. Wiley-VCH, New York.

Podbilewicz, B., E. Leikina, A. Sapir, C. Valansi, M. Suissa *et al.*, 2006 The *C. elegans* developmental fusogen EFF-1 mediates homotypic fusion in heterologous cells and in vivo. Dev. Cell 11: 471–481.

Procko, C., Y. Lu, and S. Shaham, 2011 Glia delimit shape changes of sensory neuron receptive endings in *C. elegans*. Development 138: 1371–1381.

Pujadas, L., A. Gruart, C. Bosch, L. Delgado, C. M. Teixeira *et al.*, 2010 Reelin regulates postnatal neurogenesis and enhances spine hypertrophy and long-term potentiation. J. Neurosci. 30: 4636–4649.

Rao, K., M. C. Stone, A. T. Weiner, K. W. Gheres, C. Zhou *et al.*, 2016 Spastin, atlastin, and ER relocalization are involved in axon but not dendrite regeneration. Mol. Biol. Cell 27: 3245–3256.

Rasmussen, J. P., K. English, J. R. Tenlen, and J. R. Priess, 2008 Notch signaling and morphogenesis of single-cell tubes in the *C. elegans* digestive tract. Dev. Cell 14: 559–569.

Ruschel, J., F. Hellal, K. C. Flynn, S. Dupraz, D. A. Elliott *et al.*, 2015 Systemic administration of epothilone B promotes axon regeneration after spinal cord injury. Science 348: 347–352.

Salzberg, Y., C. A. Diaz-Balzac, N. J. Ramirez-Suarez, M. Attreed, E. Tecle *et al.*, 2013 Skin-derived cues control arborization of sensory dendrites in *Caenorhabditis elegans*. Cell 155: 308–320.

Sapir, A., J. Choi, E. Leikina, O. Avinoam, C. Valansi *et al.*, 2007 AFF-1, a FOS-1-regulated fusogen, mediates fusion of the anchor cell in *C. elegans*. Dev. Cell 12: 683–698.

Sarov, M., S. Schneider, A. Pozniakovski, A. Roguev, S. Ernst *et al.*, 2006 A recombineering pipeline for functional genomics applied to *Caenorhabditis elegans*. Nat. Methods 3: 839–844.

Shemer, G., M. Suissa, I. Kolotuev, K. C. Q. Nguyen, D. H. Hall *et al.*, 2004 EFF-1 is sufficient to initiate and execute tissue-specific cell fusion in *C. elegans*. Curr. Biol. 14: 1587–1591.

Shinn-Thomas, J. H., and W. A. Mohler, 2011 New insights into the mechanisms and roles of cell-cell fusion. Int. Rev. Cell Mol. Biol. 289: 149–209.

Shinn-Thomas, J. H., J. J. Del Campo, J. Wang, and W. A. Mohler, 2016 The EFF-1A cytoplasmic domain influences hypodermal cell fusions in *C. elegans* but is not dependent on 14–3-3 proteins. PLoS One 11: e0146874.

Smith, C. J., J. D. Watson, W. C. Spencer, T. O'Brien, B. Cha *et al.*, 2010 Time-lapse imaging and cell-specific expression profiling reveal dynamic branching and molecular determinants of a multi-dendritic nociceptor in *C. elegans*. Dev. Biol. 345: 18–33.

Smith, C. J., J. D. Watson, M. K. VanHoven, D. A. Colon-Ramos, and D. M. Miller, III, 2012 Netrin (UNC-6) mediates dendritic self-avoidance. Nat. Neurosci. 15: 731–737.

Smurova, K., and B. Podbilewicz, 2016a Endocytosis regulates membrane localization and function of the fusogen EFF-1. Small GTPases 28: 1–4.

Smurova, K., and B. Podbilewicz, 2016b RAB-5- and DYNAMIN-1-mediated endocytosis of EFF-1 fusogen controls cell-cell fusion. Cell Rep. 14: 1517–1527.

Song, Y., K. M. Ori-McKenney, Y. Zheng, C. Han, L. Y. Jan *et al.*, 2012 Regeneration of *Drosophila* sensory neuron axons and dendrites is regulated by the Akt pathway involving *Pten* and microRNA *bantam*. Genes Dev. 26: 1612–1625.

Soulavie, F., and M. V. Sundaram, 2016 Auto-fusion and the shaping of neurons and tubes. Semin. Cell Dev. Biol. 60: 136–145.

Standler, N. A., and J. J. Bernstein, 1982 Degeneration and regeneration of motoneuron dendrites after ventral root crush: computer reconstruction of dendritic fields. Exp. Neurol. 75: 600–615.

Stone, C. E., D. H. Hall, and M. V. Sundaram, 2009 Lipocalin signaling controls unicellular tube development in the *Caenorhabditis elegans* excretory system. Dev. Biol. 329: 201–211.

Stone, M. C., M. M. Nguyen, J. Tao, D. L. Allender, and M. M. Rolls, 2010 Global up-regulation of microtubule dynamics and polarity reversal during regeneration of an axon from a dendrite. Mol. Biol. Cell 21: 767–777.

Stone, M. C., R. M. Albertson, L. Chen, and M. M. Rolls, 2014 Dendrite injury triggers DLK-independent regeneration. Cell Rep. 6: 247–253.

Sulston, J., and J. Hodgkin, 1988 Methods, pp. 587–606 in *The Nematode Caenorhabditis Elegans*, edited by W. B. Wood. Cold Spring Harbor Laboratory Press, Cold Spring Harbor, NY.

Tao, J., C. Feng, and M. M. Rolls, 2016 The microtubule-severing protein fidgetin acts after dendrite injury to promote their degeneration. J. Cell Sci. 129: 3274–3281.

Taylor, A. M., M. Blurton-Jones, S. W. Rhee, D. H. Cribbs, C. W. Cotman *et al.*, 2005 A microfluidic culture platform for CNS axonal injury, regeneration and transport. Nat. Methods 2: 599–605.

Taylor, C. A., J. Yan, A. S. Howell, X. Dong, and K. Shen, 2015 RAB-10 regulates dendritic branching by balancing dendritic transport. PLoS Genet. 11: e1005695.

Tkach, M., and C. Thery, 2016 Communication by extracellular vesicles: where we are and where we need to go. Cell 164: 1226–1232.

Tsalik, E. L., T. Niacaris, A. S. Wenick, K. Pau, L. Avery *et al.*, 2003 LIM homeobox gene-dependent expression of biogenic amine receptors in restricted regions of the *C. elegans* nervous system. Dev. Biol. 263: 81–102.

Valansi, C., D. Moi, E. Leikina, E. Matveev, M. Grana *et al.*, 2017 Arabidopsis HAP2/GCS1 is a gamete fusion protein homologous to somatic and viral fusogens. J. Cell Biol. 216: 571–581.

Wang, H., and E. R. Macagno, 1998 A detached branch stops being recognized as self by other branches of a neuron. J. Neurobiol. 35: 53–64.

Wang, J., M. Silva, L. A. Haas, N. S. Morsci, K. C. Nguyen *et al.*, 2014 *C. elegans* ciliated sensory neurons release extracellular vesicles that function in animal communication. Curr. Biol. 24: 519–525.

Way, J. C., and M. Chalfie, 1989 The mec-3 gene of Caenorhabditis elegans requires its own product for maintained expression and is expressed in three neuronal cell types. Genes Dev. 3: 1823–1833.

Wehman, A. M., C. Poggioli, P. Schweinsberg, B. D. Grant, and J. Nance, 2011 The P4-ATPase TAT-5 inhibits the budding of extracellular vesicles in *C. elegans* embryos. Curr. Biol. 21: 1951–1959.

White, J., K. Matlin, and A. Helenius, 1981 Cell fusion by semliki forest, influenza, and vesicular stomatitis viruses. J. Cell Biol. 89: 674–679.

White, J. G., E. Southgate, J. N. Thomson, and S. Brenner, 1986 The structure of the nervous system of Caenorhabditis elegans. Philos. Trans. R. Soc. Lond. B Biol. Sci. 314: 1–340.

Wu, Z., A. Ghosh-Roy, M. F. Yanik, J. Z. Zhang, Y. Jin *et al.*, 2007 *Caenorhabditis elegans* neuronal regeneration is influenced by life stage, ephrin signaling, and synaptic branching. Proc. Natl. Acad. Sci. USA 104: 15132–15137.

Yan, D., Z. Wu, A. D. Chisholm, and Y. Jin, 2009 The DLK-1 kinase promotes mRNA stability and local translation in *C. elegans* synapses and axon regeneration. Cell 138: 1005–1018.

Yanik, M. F., H. Cinar, H. N. Cinar, A. D. Chisholm, Y. Jin *et al.*, 2004 Neurosurgery: functional regeneration after laser axotomy. Nature 432: 822.

Yaniv, S. P., N. Issman-Zecharya, M. Oren-Suissa, B. Podbilewicz, and O. Schuldiner, 2012 Axon regrowth during development and regeneration following injury share molecular mechanisms. Curr. Biol. 22: 1774–1782.

Yassin, L., B. Gillo, T. Kahan, S. Halevi, M. Eshel *et al.*, 2001 Characterization of the DEG-3/DES-2 receptor: a nicotinic acetylcholine receptor that mutates to cause neuronal degeneration. Mol. Cell. Neurosci. 17: 589–599.

Yip, Z. C., and M. G. Heiman, 2016 Duplication of a single neuron in *C. elegans* reveals a pathway for dendrite tiling by mutual repulsion. Cell Rep. 15: 2109–2117.

Communicating editor: M. V. Sundaram